Chaos, Solitons and Fractals 139 (2020) 109973

Contents lists available at ScienceDirect

Chaos, Solitons and Fractals

Nonlinear Science, and Nonequilibrium and Complex Phenomena

journal homepage: www.elsevier.com/locate/chaos

Travel time analysis in the Chinese coupled aviation and high-speed rail network

Yiqiao Wang[a,b], Qiaoyi Lu[a], Xianbin Cao[a,b], Xuesong Zhou[c], Vito Latora[d,e], Lu Carol Tong[b,f,*], Wenbo Du[a,b,*]

[a] School of Electronic and Information Engineering, Beihang University, Beijing 100191, PR China
[b] National Engineering Laboratory for Comprehensive Transportation Big Data Application Technology, Beijing 100191, PR China
[c] School of Sustainable Engineering and the Built Environment, Arizona State University, Tempe, AZ, 85287, USA
[d] School of Mathematical Sciences, Queen Mary University of London, London E1 4NS, UK
[e] Dipartimento di Fisica ed Astronomia, Università di Catania and INFN, I-95123 Catania, Italy
[f] Research Institute of Frontier Science, Beihang University, Beijing 100091, PR China

ARTICLE INFO

Article history:
Received 26 November 2019
Revised 30 May 2020
Accepted 4 June 2020

Keywords:
Coupled aviation and high-speed rail network
Complex network
Travel time analysis

ABSTRACT

Thanks to the rapid expansion of the Chinese Aviation (A) network and of the High-Speed Rail (HSR) network, intermodal travel across air transport and the high-speed rail network has become a fully integrated process for many inter-city travelers. By constructing the spatially-embedded Coupled Aviation and High-Speed Rail (CAHSR) network, whose two layers respectively represent the aviation and the HSR network, while the coupling describes ground transfer between different facilities (airports and/or rail stations) in the same city, we focus on a systematic travel time analysis for major mega-regions. Our empirical analysis calculates passengers' end-to-end travel time between major mega-regions, including real information on waiting and transfer time. The results indicate that sufficient frequencies of flights/HSR trains have led to high multi-modal accessibility across different time periods of the day. In addition, we also find that highly intermodal air-HSR mobility pathways can be extremely important to link small cities to urban mega-region hubs. Our findings may assist timetable improvement in future infrastructure planning for the CAHSR network.

© 2020 Elsevier Ltd. All rights reserved.

1. Introduction

With the further development of reform and opening-up as well as the globalization process, China has become more involved in international economic activities, and the rapid growth of its economy has maintained a good momentum [35]. Economic prosperity has always been dependent on accelerated development of national-level transportation networks. As fundamental components of inter-region transportation systems, aviation and high-speed rail (HSR) have attracted lots of attention and experienced sustained, rapid evolution.

For the last decade, Chinese air transportation volume has ranked the second in the global air transportation market, with 612 million passengers and 7.385 million tons of freight in 2018 [26]. By 2025, the nation-wide air transportation network will cover 93.2% of prefecture-level cities and 89% of counties. Aviation services will be responsible for the mobility of 92% of the population. [27].

In addition to air transport, HSR provides another form of convenient medium-to-long distance transportation service. The Chinese high-speed railway system has made great strides since the first high-speed railway came into operation in 2008. After a short span of ten years' development, Chinese high-speed rail mileage now exceeds 29,000 kilometers, surpassing the high-speed rail mileage of all other countries in the world. According to the newly revised "National Medium and Long-Term Railway Network Plan", high-speed railway mileage will reach 38,000 kilometers by 2025, and the high-speed railway network will basically cover all provincial capitals and other large and medium-sized cities with a population of more than 500,000 in 2030 [28].

As aviation and HSR transport possess unique technical and economic characteristics, they have attracted the attention of a wide range of scholars and experts. Their complex relationship has aroused great interest as a key issue in existing studies. Initially, researchers considered the relationship of aviation with high-speed rail as either a competition [9] or a cooperation [22]. After years of study, increasing numbers of researchers have reached a tacit

* Corresponding authors.
E-mail addresses: ltong@buaa.edu.cn (L.C. Tong), wenbodu@buaa.edu.cn (W. Du).

https://doi.org/10.1016/j.chaos.2020.109973
0960-0779/© 2020 Elsevier Ltd. All rights reserved.

agreement that competitive relationships coexist with cooperative ones [1,40]. Albalate et al. [1] find HSR competes with airlines in terms of air service frequencies and seats, while it also plays an intermodal complementary role for airlines in different regions. By analyzing the effects of competition between aviation and HSR from various aspects, Xia and Zhang [40] show that such a competition may lead to higher airfare where HSR services are inaccessible, while cooperation could possibly be more beneficial on the routes where terminal airport capacity is extremely tight. Yang et al. [41] compare the spatial configuration of aviation with HSR in the Chinese national urban system based on passenger origin/destination (OD) data. The analysis shows that cities that depend more on HSR are located mainly in the middle and eastern parts of China; by contrast, the aviation-dominant cities, connected through interregional services, are distributed across the whole country. Along this research line, Zhu et al. [42] establish a dynamic weighted model to measure the air/rail intercity transportation connectivity in China. They point out that international trips are usually conducted by air transport, and depend on several major airports in particular. Meanwhile, compared to airlines, HSR is a dominant option for domestic routes up to 1300 km and serves more than 80% of top-ranking domestic routes.

In the past few decades, complex network theory has gained a large amount of attention from various scientific communities [4,10,24,29,34], such as network modeling [6,31,38], information traffic [37], and cascading failures [17,39]. It is noteworthy that complex network theory has been widely used in large-scale transportation network analysis, especially in aviation and railways. The concept of complex networks has been extensively applied in air transportation networks (ATN) [7,14,16]. Meanwhile, complex network theory plays a crucial role in railway network research [32]. In recent years, the study of coupled networks has been considered an important research area [5,8,25,33]. From a theoretical view, the Chinese aviation and high-speed rail network is a coupled network in nature, so a coupled network modeling framework is of great help to investigate interconnected infrastructures/facilities and their underlying relationship [3,13,23].

In this paper, based on the framework of coupled networks, we develop a timetable-based modeling approach to incorporate critical temporal factors into the travel time analysis [2,19,20]. By combining the two transportation modes into the Coupled Aviation and High-Speed Rail (CAHSR) network, where nodes denote cities and edges denote flights or HSR trains between cities, we fully analyze travelling performance and efficiency in the CAHSR network of 265 cities. We also investigate the impact of departure time on travel time for different cities. The results show that for large cities, due to the high density of flights/HSR trains operating each hour, travel time are usually short and the choice of departure time is relatively flexible, while the opposite result is found for the small cities. Finally, we examine the dependence and robustness properties of the CAHSR network.

The paper is organized as follows. In Section 2, we describe the framework to model the Coupled Aviation and High-Speed Rail network and we introduce the basic quantities and metrics that will be used to characterize its spatio-temporal properties. The results of the empirical analysis of the CAHSR network structure on the travel time and on intermodal dependence and robustness properties of the network are reported and discussed in Section 3. The final conclusions are drawn is Section 4.

2. Methodology

2.1. Modeling the CAHSR network

We model the integrated air transport and high-speed rail system in China as a spatially-embedded coupled network with two layers, respectively representing the Aviation network (A) and the High-Speed Rail (HSR) network, and a coupling between the two layers that describes ground transfer between different facilities (i.e. from one airport to another airport, from one airport to a rail station, or from one rail station to another station) within a city. The coupled network that we get, $M = \{G_A, G_H, C\}$, named Coupled Aviation and High-Speed Rail (CAHSR) network, thus consists of graph G_A, describing the topology of the aviation network, graph G_H, describing the topology of the HSR network, and graph C representing the ground transfer connections between airports and HSR stations within a city. The nodes of our coupled networks are major Chinese cities, i.e. cities with air and/or HSR services. Consequently, the network has three different types of nodes, namely aviation nodes, corresponding to cities with only airports, HSR nodes, corresponding to cities with only HSR stations, and coupling nodes, denoting cities with both airports and HSR stations, where it is therefore possible to change mode of transportation. When at least one flight or one HSR train travels from city i to city j, an edge (i, j) is built between the two cities/nodes. It should be noted that if a passenger arrives at any airport or HSR station in a given city, it indicates that the passenger arrives in the city.

Fig. 1 provides an illustrative example of an air/HSR network with five cities, where city A is a coupling city with two airports (a1 and a2) and two HSR stations (r1 and r2), city B (with airports a3 and a4) and city C (with an airport a5) are aviation cities, and city D (with HSR stations r3 and r4) and city E (with HSR station r5) are HSR cities. There are three types of edges. Light blue edges represent direct air services between different cities. Similarly, the HSR services are denoted by dark blue edges. In addition, for cities with multiple transportation facilities, such as cities A, B, and D, the ground transfer links between airports and rail stations (a-r), different airports(a-a) and different rail stations (r-r) within a city are shown in red, light purple, dark purple, respectively.

2.2. Travel time analysis of the CAHSR network

In daily medium-to-long distance travel, the end-to-end travel time is one of the major concerns for all passengers. For each travel from a city i to a destination city j, we can define the total travel time t_{ij} along the path with the shortest possible time. Typically, the total travel time t_{ij} from source to destination consists of three component parts, namely in-vehicle (i.e. in-flight or in-rail travel time) t^V, transfer time t^T (including the exiting/entering time and ground transfer time), and waiting time at airports/stations t^W. Each of these three time represents the total time in the corresponding category (e.g. transfer time t^T is the sum of the times of each of the transfers in a given travel). Hence the total travel time t between any given city pair can be calculated as in Eq. (1):

$$t = t^V + t^T + t^W \tag{1}$$

Flight/HSR travel time t^V reflects the actual travel time spent on flights/trains and primarily depends on the distance to the desired destinations as well as the technical/operating speed of the flight/HSR. This can be obtained from the published timetables/schedules. Transfer time t^T needs to be considered when the passenger has to visit an intermediate transfer facility, which includes exiting/entering time of transportation facilities and ground transfer time. t^T always determined by the service level of airports/HSR stations and urban planning. Generally, an efficient trip is largely decided by the redundant waiting time t^W at the departure airport/station or for the consecutive trip, which is affected by the synchronization of timetables. Obviously, both t^V and t^T are limited to objective factors that cannot be easily changed, while the fluctuation of t^W is mainly caused by incoordination between different timetables. When the impact of different departure time

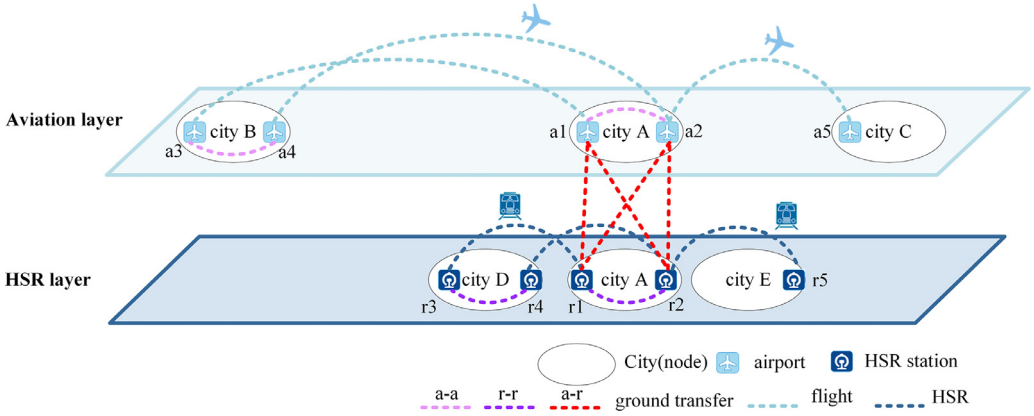

Fig. 1. An illustrative air/HSR multilayer network.

needs to be considered, t^W also represents the waiting time at the beginning of trips.

As shown in Fig. 1, if a passenger travels from city C to city D, the total travel time t_{CD} can be represented as in Eq. (2):

$$t_{CD} = t_C^W + t_{CA}^V + t_A^T + t_A^W + t_{AD}^V \tag{2}$$

The following three quantities, namely the average total travel time t_i, the average number of transfers n_i, and proportions of the three travel time components, will be considered to describe the transportation features of a city i in the CAHSR network.

1) Average total travel time t_i

The average total travel time t_i indicates the expected travel time to all the other cities j in the network and is defined in Eq. (3), where t_{ij} is the total travel time from node i to node j, and the sum are taken over all the N cities in the network.

$$t_i = \frac{1}{N}\sum_j t_{ij} \tag{3}$$

2) Average number of transfers n_i

The average number of transfers n_i can be calculated by Eq. (4).

$$n_i = \frac{1}{N}\sum_j n_{ij} \tag{4}$$

3) Proportions of the three travel time components

As described in the previous subsection, the total travel time t_{ij} can be divided into three components, namely in-vehicle travel time t_{ij}^V, transfer time t_{ij}^T, and waiting time t_{ij}^W. It should be noted that the transfer time t_{ij}^T and the waiting time t_{ij}^W represent the summation of transfer time and waiting time for the departure city and all possible intermediate cities along the trip. The corresponding proportions, i.e., in-vehicle travel time proportion p_i^V, transfer time proportion p_i^T, and waiting time proportion p_i^W are defined in equations (5).

$$\begin{aligned} p_i^V &= \tfrac{1}{N}\textstyle\sum_j \frac{t_{ij}^V}{t_{ij}} \\ p_i^T &= \tfrac{1}{N}\textstyle\sum_j \frac{t_{ij}^T}{t_{ij}} \\ p_i^W &= \tfrac{1}{N}\textstyle\sum_j \frac{t_{ij}^W}{t_{ij}} \end{aligned} \tag{5}$$

To explicitly show the components of each travel time, all possible travel modes including two direct travel modes and six transfer modes are defined in Fig. 2 using the cities and transportation network in Fig. 1. For the direct travel mode by which passengers travel via only airline or HSR (e.g., from airport a1 to a3, from HSR station r1 to r3), total travel time t is equal to the flight/rail travel time t^V plus departure waiting time t^W. If there are no suitable direct flight/train routes, transfers cannot be avoided. Thus, additional transfer time t^T and waiting time t^W should be taken into account at the intermediate facilities. In transfer travel modes 1 and 2, passengers can transfer in the same airport/HSR station without extra time spending on the ground traffic.

When passengers need to travel between different facilities in one city (transfer travel modes 3, 4, 5, and 6), as the transfer links in modes 3 and 4 are shown in light purple and dark purple. Specifically, the last two modes (modes 5 and 6) relate to more than one transport mode and only exist in coupling cities are shown as red links.

2.3. Space-time analysis of the CAHSR network

To further understand the patterns of travels from origin to destination in the CAHSR network, we analyze travels that start at different time of the day. Notice, in fact, that the shift of passenger departure time may lead to very different total travel time due to alternative connections available. Consider the following illustrative example in Fig. 1, where two passengers traveling from city E to city B are considered to be departing at time $\tau 1$ and $\tau 2$ respectively. As shown in Fig. 3, passenger 1 departs from HSR station r5 at time $\tau 1$ and reaches city A at time $\tau 3$. After the ground transfer time, this passenger is able to catch the flight taking off at time $\tau 5$ from city A to city B. Conversely, passenger 2, who takes the HSR train from city E to city A at $\tau 2$, misses the flight to city B at $\tau 5$; thus, he/she has to wait an additional period of time for the next flight and eventually arrives at city B at $\tau 8$. The total travel time for passenger 2 is $(\tau 8 - \tau 2)$, which is much longer than passenger 1's total travel time $(\tau 7 - \tau 1)$.

Typically, there are many routes from one city to the others. In this paper it is assumed that least time-consuming routes are selected. Similar to equations (1), the total travel time t_{ij}^q of a travel departing at time q can be calculated by Eq. (6):

$$t_{ij}^q = t_{ij}^{V,q} + t_{ij}^{T,q} + t_{ij}^{W,q} \tag{6}$$

3. Data and results

3.1. The CAHSR network

The flight data used in this paper are obtained from the Air Traffic Management Bureau (ATMB) of China. As of June 17, 2016, the domestic flight schedule contains 11,087 flights. The data for the HSR are provided by China Railway Corporation. The schedule

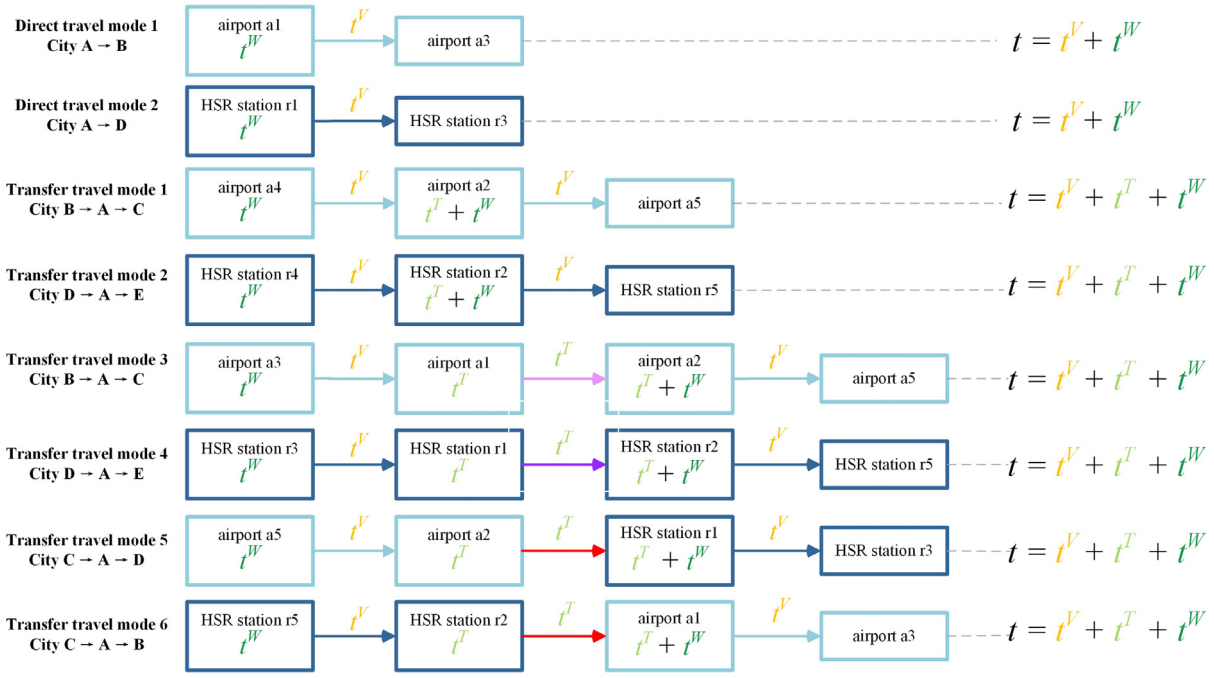

Fig. 2. All travel modes with two direct travel modes and six transfer modes.

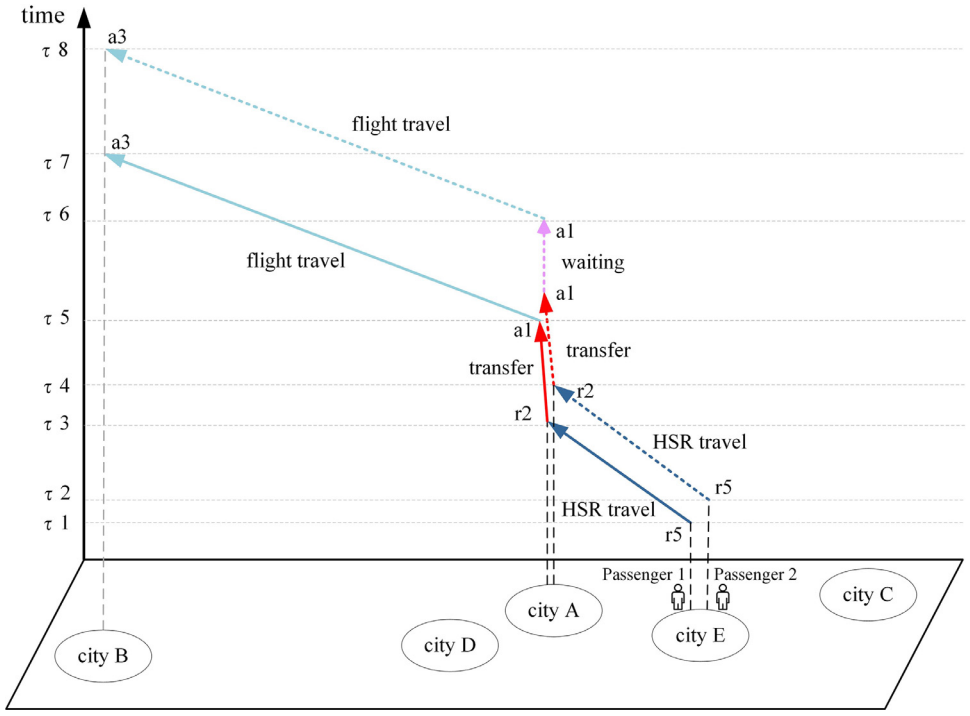

Fig. 3. Passenger space-time trajectories in the CAHSR network. Dark blue lines are the HSR train routes, light blue lines are the aviation routes, the red lines are the ground transfer, and the light purple line represent waiting time at the airport a1. (For interpretation of the references to color in this figure legend, the reader is referred to the web version of this article.).

for the G prefix trains on June 17, 2016 contains 1716 G-class trains. The exiting/entering time are obtained from the literature [43]. Ground transfer time within a city are extracted from Google's Distance Matrix [18], which provides the estimated shortest travel time between any two airports/HSR stations in the same city.

Based on this flight and train schedule data, a CAHSR network with 200 airports and 387 HSR stations has been constructed. The airports and HSR stations are located in 265 cities/nodes, including 4 municipalities, 257 prefecture-level cities, and 4 provincial-controlled divisions. According to their transportation modes, these cities can also be divided into 114 aviation cities, 84 HSR cities, and 67 coupling cities. Most of the aviation cities, all HSR cities, and all coupling cities are located in the eastern and central parts of China,

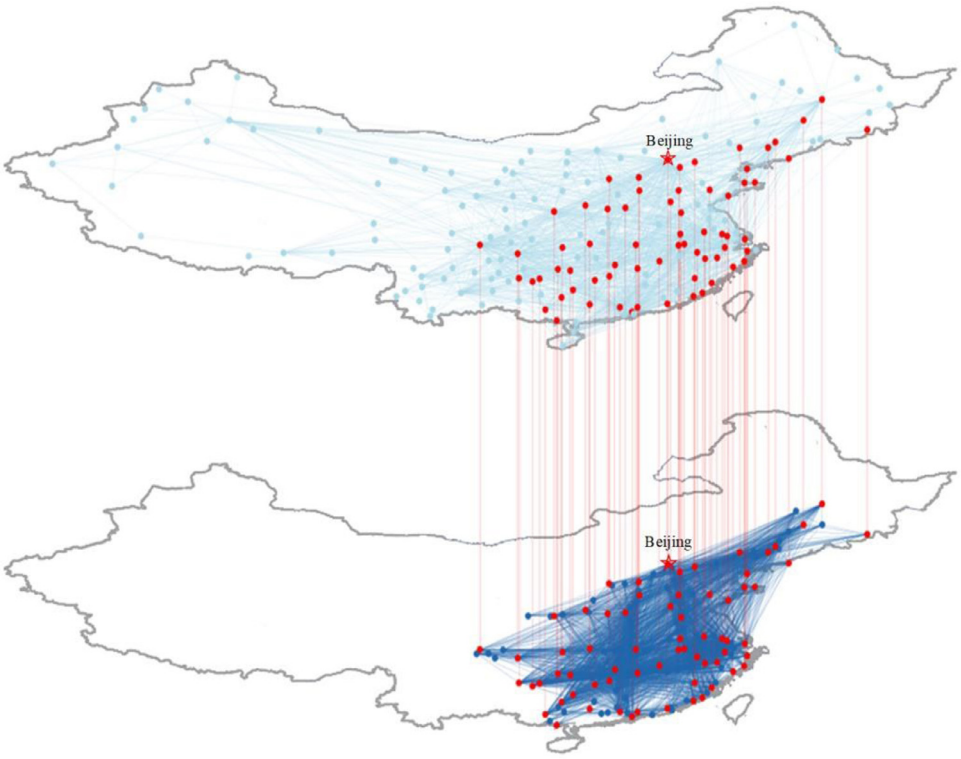

Fig. 4. The structure of the CAHSR network. Red dots are the coupling cities, i.e. cities where both airports and HSR stations are present, light blue dots are the aviation cities, and dark blue dots are the HSR cities. The red lines represent the ground transfer between airports and HSR stations in the coupling cities, the light blue lines represent the aviation edges, and the dark blue lines represent the HSR edges. (For interpretation of the references to color in this figure legend, the reader is referred to the web version of this article.).

Table 1
Topology parameters of the three networks.

	Mean of degree k	Mean of weight w	Clustering coefficient C	Average shortest path length L	Degree heterogeneity H	Degree assortativity coefficient r	Mean of density d
Aviation network	17.083	61.160	0.701	2.122	2.704	−0.444	0.010
HSR network	51.358	97.470	0.736	1.692	1.230	−0.060	0.368
CAHSR network	38.374	97.313	0.725	2.014	1.898	−0.250	0.154

while in contrast, only a small number of aviation cities are in the west.

Fig. 4 illustrates the structure of the CAHSR network. The upper layer is the aviation network containing aviation cities and coupling cities, with a total of 181 nodes and 1545 edges. The lower layer is the HSR network including HSR cities and coupling cities, with a total of 151 nodes and 3878 edges. By means of the ground transfer in coupling cities (red lines in Fig. 4), the aviation network and HSR network are coupled together to form the CAHSR network, with a total of 265 nodes.

3.2. Network properties of the CAHSR network

To characterize the structure of the CAHSR network, we have first investigated some basic node quantities, such as the degree k, the weight w, the clustering coefficient C, and some network metrics such as the shortest path length L, the degree heterogeneity H, and the degree assortativity coefficient r [11,21,30,36]. Detailed definitions are provided in the Appendix.

The obtained results for the aviation network (with both aviation cities and coupling cities), the HSR network (with both HSR cities and coupling cities), and the CAHSR network (with all aviation cities, HSR cities, and coupling cities) are reported in Table 1. The node degree k and weight w are two parameters that reflect the number of direct connecting cities and departing flights/HSR trains, respectively. We notice that the average degree k of the HSR network is significantly higher than that of the other two networks. The average weight w of the CAHSR network which takes traffic flows into account is as high as that of the HSR network. The three networks all have small-world network characteristic according to their relatively large clustering coefficient C (from 0.701 to 0.736) and small average shortest path length L (from 1.692 to 2.122). We also measure the variance of node degrees. The aviation network has the highest degree heterogeneity of 2.704, as the difference among its node degrees is greater than in the other two networks. The large disassortative behavior of the aviation network demonstrates that large-degree cities tend to connect to small degree cities, showing strong scale-free property. Negative degree assortativity coefficients indicate that all three networks are disassortative networks. The large disassortative behavior (absolute value of −0.444) of the aviation network demonstrates that in this system large-degree cities tend to connect to cities with small degree. The density d of the HSR network is 0.36848, which is approximately thirty-eight times higher than that of the aviation network and three times higher than that of the CAHSR network. It can be interpreted that HSR cities are concentrated in the central and eastern China with small disassortative behavior, while the aviation cities have large degree heterogeneity behavior and distributed throughout the country.

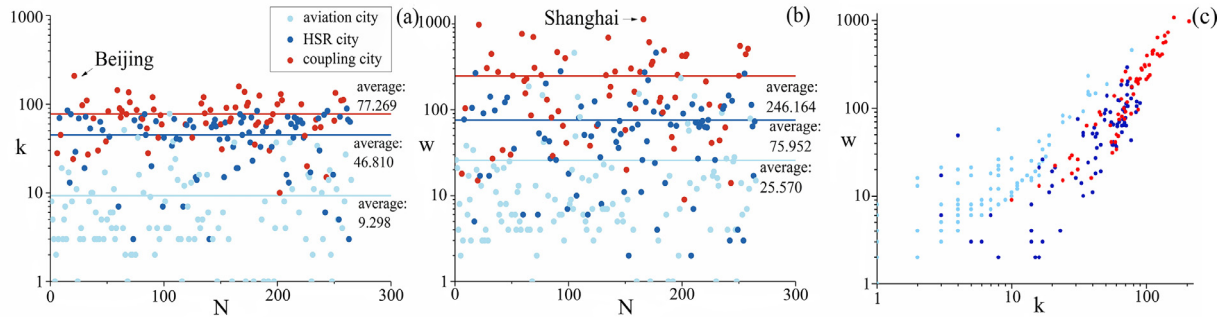

Fig. 5. (a) Degree k and (b) weight w for each of the N, where N represent the city number indicator. (c) Distribution of k/w. The three types of cities are shown in different colors. (For interpretation of the references to color in this figure legend, the reader is referred to the web version of this article.).

Table 2
Topology parameters of the three types of cities.

	Average degree k	Average weight w	Betweenness centrality B	Clustering coefficient C	Average shortest path length L
Aviation cities	9.298	25.570	0.00114755	0.769	2.207
HSR cities	46.810	75.952	0.00087514	0.767	1.945
Coupling cities	77.269	246.164	0.01220067	0.596	1.743

Fig. 5 further displays the topological characteristics in terms of different city types (aviation cities, HSR cities, and coupling cities). HSR cities are generally higher in degree k and weight w than those of the aviation cities, which is consistent with the phenomenon observed in the network analysis. Among all cities, the city with the highest k is Beijing, and the city with the highest w is Shanghai. The average degree k of aviation cities is 9.298, while the average degree of HSR cities is approximately five times larger than that of aviation cities. Meanwhile, the average weight w of HSR cities is roughly three times larger than that of aviation cities. Moreover, coupling cities play a critical role in connecting aviation cities and HSR cities, and the average k and w of coupling cities are apparently much higher than those of the other two types of cities.

The correlation between nodes with different k and w are shown in Fig. 5(c). The correlation coefficients of k and w are 0.896, 0.784 and 0.929 in aviation cities, high-speed rail cities, and coupling cities respectively. Moreover, the average k and w of coupling cities are apparently higher than those of the other two types of cities. Both coupling cities and aviation cities have a strong $k-w$ correlation and the coupling cities show highest $k-w$ correlation. Furthermore, for large degree coupling cities, the frequency of daily flights/HSR trains is much higher than that of aviation cities and HSR cities.

Table 2 shows several basic topology parameters, i.e., degree, weight, betweenness centrality, clustering coefficient, and average shortest path length. Betweenness centrality B denotes the proportion of the shortest paths that contain a given node. The coupling cities have an average betweenness centrality of 0.0122, roughly ten times higher than that of HSR cities and aviation cities, which shows that coupling cities include more important nodes on their shortest paths. The reason can be interpreted as the fact that the adjacent nodes of the coupling cities can be either aviation cities or HSR cities, while aviation cities and HSR cities cannot be directly connected to each other. Moreover, coupling cities play a more pivotal role in transfers, as many cities use coupling cities as their transfer stations to connect to other cities. The average shortest path length L shows the number of transfers required to reach the rest of the network from those three cities. The aviation cities has the highest L (2.207) while the coupling cities has the least L (1.743).

3.3. Travel time analysis of the CAHSR network

The total travel time is the most critical factor affecting passengers' travel choices. In order to explore the travel time characteristics of the CAHSR network, in this section we provide quantitative results relative to two different aspects of the problem. Firstly, we calculate the shortest-time paths (i.e. shortest paths in terms of total spent time) between any two cities with intermodal transfers taken into account, and we study the specific patterns of such paths for different city types. Secondly, considering the time-varying nature of the CAHSR network, we also study the variation of travel time under different departure time.

3.3.1. Analysis of shortest travel time paths

For each city, we calculate its total travel time to all the other 264 cities based on the equations in Section 2. Fig. 6 shows distributions of average total travel time, average number of transfers, and corresponding travel time proportions. The coupling cities show obvious advantages in both travel time and number of transfers. It can be observed that the average total travel time t ranges from four to nine hours and the number of transfers n ranges from 0.5 to 1.6, which are both significantly smaller than the corresponding values for the other two types of cities. By comparison, when a passenger's origin is an aviation/HSR city, he/she may take nine to twelve hours to reach the "farthest" city. Coupling cities' highest proportion p^V of in-vehicle travel time also indicates that travel originating from coupling cities is relatively convenient with less transfer time and waiting time due to the fact that these cities have the highest degree and highest weight. This phenomenon can be understood by their geographical locations, given in Fig. 4. All coupling cities are concentrated in the eastern or central region, consisting of major municipalities and most provincial capitals with important political status and high levels of economic prosperity. Table 3 provides the top three and last three cities in terms of minimum total travel time, minimum number of transfers, and maximum proportion of in-vehicle travel time. The national capital city, Beijing, and the financial center, Shanghai, demonstrate good performance as expected. On the opposite, the last three cities are all aviation cities with limited transportation resources located far away from central China.

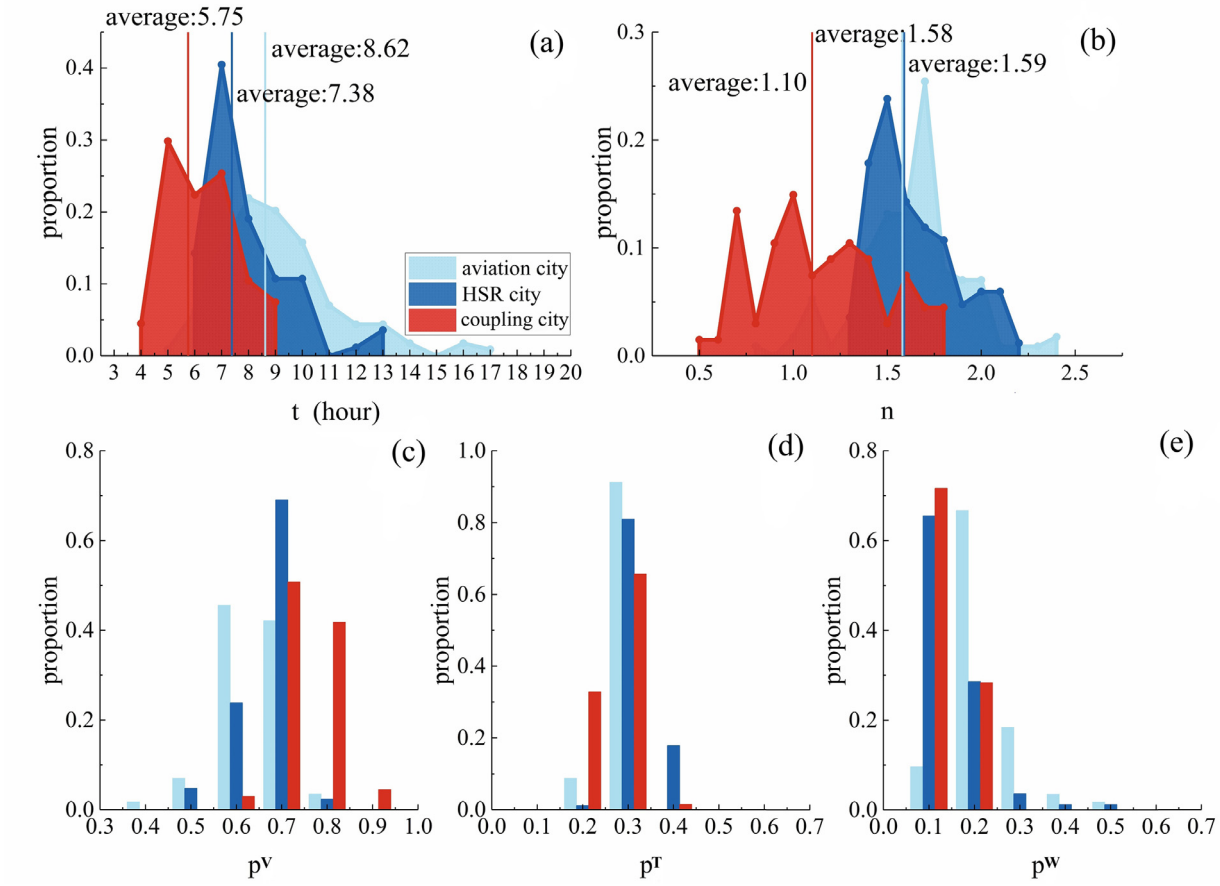

Fig. 6. (a) Distribution of total travel time t. (b) Distribution of number of transfers n.
(c) Distribution of in-vehicle travel time proportion p^V. (d) Distribution of transfer time proportion p^T. (e) Distribution of waiting time proportion p^W.

Table 3
Top three and bottom three cities in terms of minimum travel time t, minimum number of transfers n, and maximum time proportion p^V of in-vehicle travel time.

Rank	t	n	p^V
1	Beijing	Beijing	Beijing
2	Shanghai	Shanghai	Shanghai
3	Xi'an	Hangzhou	Guangzhou
263	Ali	Heihe	Hechi
264	Yichun	Ali	Jinchang
265	Turpan	Turpan	Zhangye

3.3.2. Dependence on different departure time

Due to aviation/HSR schedules, passengers' travel time may vary considerably given different departure time. To further discuss the impact of departure time, a day is evenly divided into 24 time intervals, i.e., interval 1 of 0:00–1:00, interval 2 of 1:00–2:00, and so on. Although passengers could depart at any time interval during a day, we choose the beginning of the aforementioned intervals for simplicity.

Fig. 7(a) indicates that average total travel time at different departure time intervals in the CAHSR network changes throughout the day. As the fluctuation of T is larger than the fluctuation of t^V and t^T, the variation of t^W is the main factor leading to the difference in the $t-T$ distribution. Passengers have to spend some time (included in t^W) waiting for flights or HSR trains at the beginning of their trips. For cities with larger w, the likelihood of a long waiting time at the departure airport/station is relatively small; while for cities with smaller w, the time spent in waiting may potentially increase. Therefore, weight w reflects the frequency of timetables and greatly affects total travel time at different time intervals.

The characteristics of cities within 24-time intervals mainly depend on the time-varying nature of the whole network. As shown in Fig. 7(a), the distribution of average total travel time t over the entire network in each 24 time intervals forms a "V" shape, in which the lowest time point is around interval 9:00am. Generally, in the CAHSR network, the optimal departure time should be somewhere within intervals 7:00am to 10:00am. Fig. 7(b) shows that the mean and variance of the total travel time increases with decreasing weight w. For cities with large weight, due to the high density of flights/HSR trains, total travel time are short and the decision to select different departure time may not lead to additional waiting time. However, when passengers travel from a small-weight city, they only have limited choices for departure time.

In order to explore the impact of weight w on each city's travel efficiency, three typical cities are further studied, namely Guangzhou (capital city, w=765, rank 3), Huizhou (mid-scale city, w=29, rank 133), and Yunfu (small-scale city, w=3, rank 245). These three cities are chosen from the same province (Guangdong) to avoid the interference caused by geographical locations and other factors.

In Fig. 8, the three cities' mean and variance of total travel time t progressively increase as their weights decrease. Similar to Fig. 7, in-vehicle travel time t^V and transfer time t^T of the three cities are essentially the same, and the main cause for the fluctuations of t in different time intervals is the variations of t^W. The optimal departure time of the three cities is around 9:00am, which is accord with the whole network distribution in Fig. 7(a); however, there are great differences in the distribution of the three cities. The average total travel time from Guangzhou to the whole network is the smallest with the least fluctuation. However, when traveling

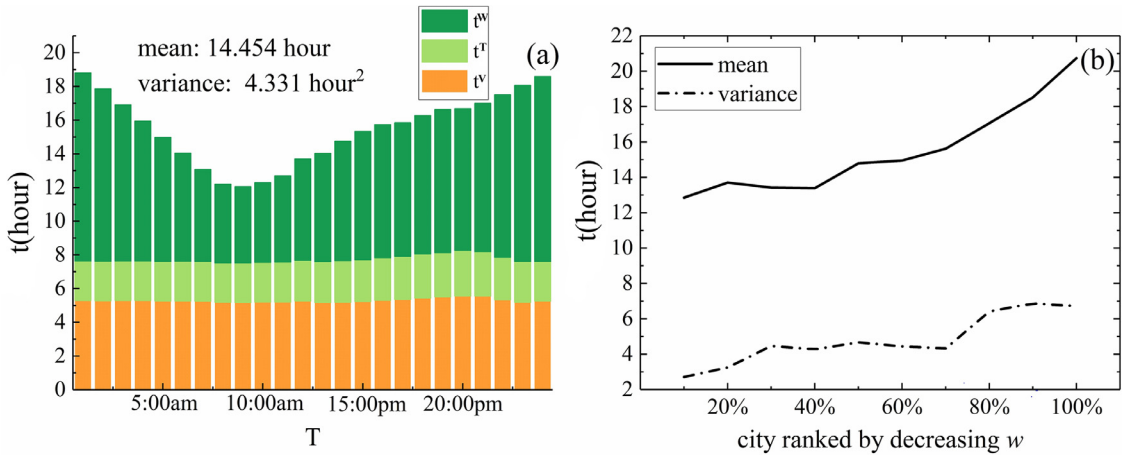

Fig. 7. (a) Average total travel time of the CAHSR network during a day. (b) The variation of mean and variance of the total travel time increases with decreasing weight *w*. Cities are listed from large values of *w* to small values, i.e., 10% represents the top 10% of cities in terms of weight *w*.

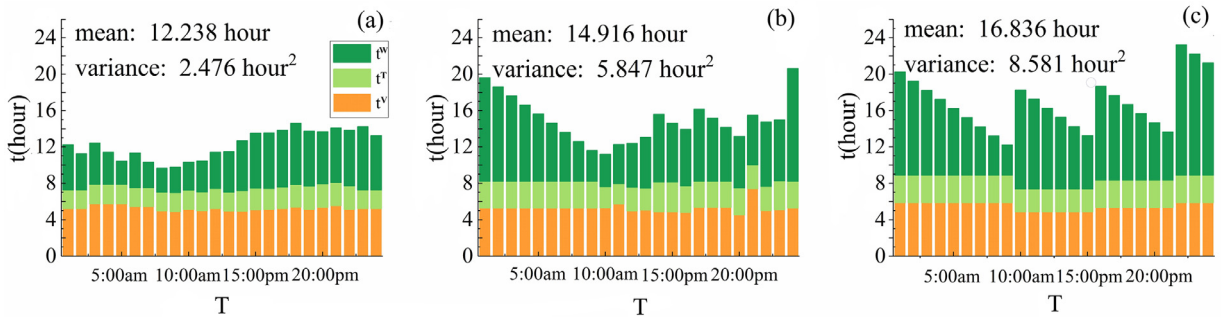

Fig. 8. (a) The average *t* for Guangzhou at different time intervals. (b) The average *t* for Huizhou at different time intervals. (c) The average *t* for Yunfu at different time intervals.

from the HSR city Yunfu, passengers' mobility is reduced because there are only three HSR trains departing at 9:00am, 15:00pm, and 21:00pm each day. For the mid-scale city Huizhou, the fluctuation in total travel time is between that of the other two cities. Therefore, for cities with large *w*, due to the large number of flights/trains, travel time are usually short and not depending on the choice of the departure time. The result for small-weight cities is the opposite, and in this case the choice of the departure time can greatly affect the resulting travel times. These findings may help improve the CAHSR system performance by optimizing intermodel schedules. Optimizing time schedules in those small-scale cities could be of great value for reducing total travel time.

3.4. Analysis of the inter-dependence of the air and the HSR network

The CAHSR network provides high-quality services by relying on both the aviation network and the HSR network. The seamless cooperation of aviation and HSR offers more flexible intermodal travel options improving the overall efficiency of the integrated transportation system. This subsection analyzes how travels depend on the two different transportation modes of the CAHSR network.

3.4.1. Intermodal travel in the CAHSR network

In the CAHSR network, all desired routes can be divided into three categories: aviation routes and HSR routes (where passengers carry out their travel activities through either airlines or HSR alone), and integrated routes (where passengers need to use both airlines and HSR to reach their destinations). The percentage of integrated routes directly reflects the dependence of schedules on the cooperation of the two transportation modes. By proposing an intermodal dependence coefficient, we evaluate the intermodal travel dependence of different cities.

The percentage of aviation routes p_{Ai}, HSR routes p_{Hi}, and integrated routes p_{Ci} from city i are defined in Eqs. (7-9), where AR_i, HR_i, and CR_i are the number of aviation routes, HSR routes, and integrated routes on the time-saving paths to all other cities from city i. R_i denotes the number of routes from city i to all the other cities, and for any i there is $P_{Ai} + P_{Hi} + P_{Ci} = 1$.

$$p_{Ai} = \frac{AR_i}{R_i} \tag{7}$$

$$p_{Hi} = \frac{HR_i}{R_i} \tag{8}$$

$$p_{Ci} = \frac{CR_i}{R_i} \tag{9}$$

Fig. 9 demonstrates the geographical distribution of cities that strongly depend on aviation and HSR, respectively. As shown in Fig. 9(a), cities with a high percentage of aviation routes p_A (0.62–0.65) are coupling cities or aviation cities, and are scattered widely across the whole nation, with a greater concentration along the southwest border. In contrast, cities with the highest percentage of HSR routes p_H are mostly HSR cities and are mainly located in the eastern region of China, as shown in Fig. 9(b).

Some cities benefit more from intermodal services through transfers in coupling cities. For instance, Qinzhou's percentage of integrated routes p_{Ci} is 0.89. That is to say, nine out of ten least time routes rely on the cooperation of two transportation modes. Fig. 10 displays the geographical distribution of fifteen cities with the highest p_C (0.72–0.89). These cities are almost all HSR cities, and eleven of them belong to urban agglomerations proposed in

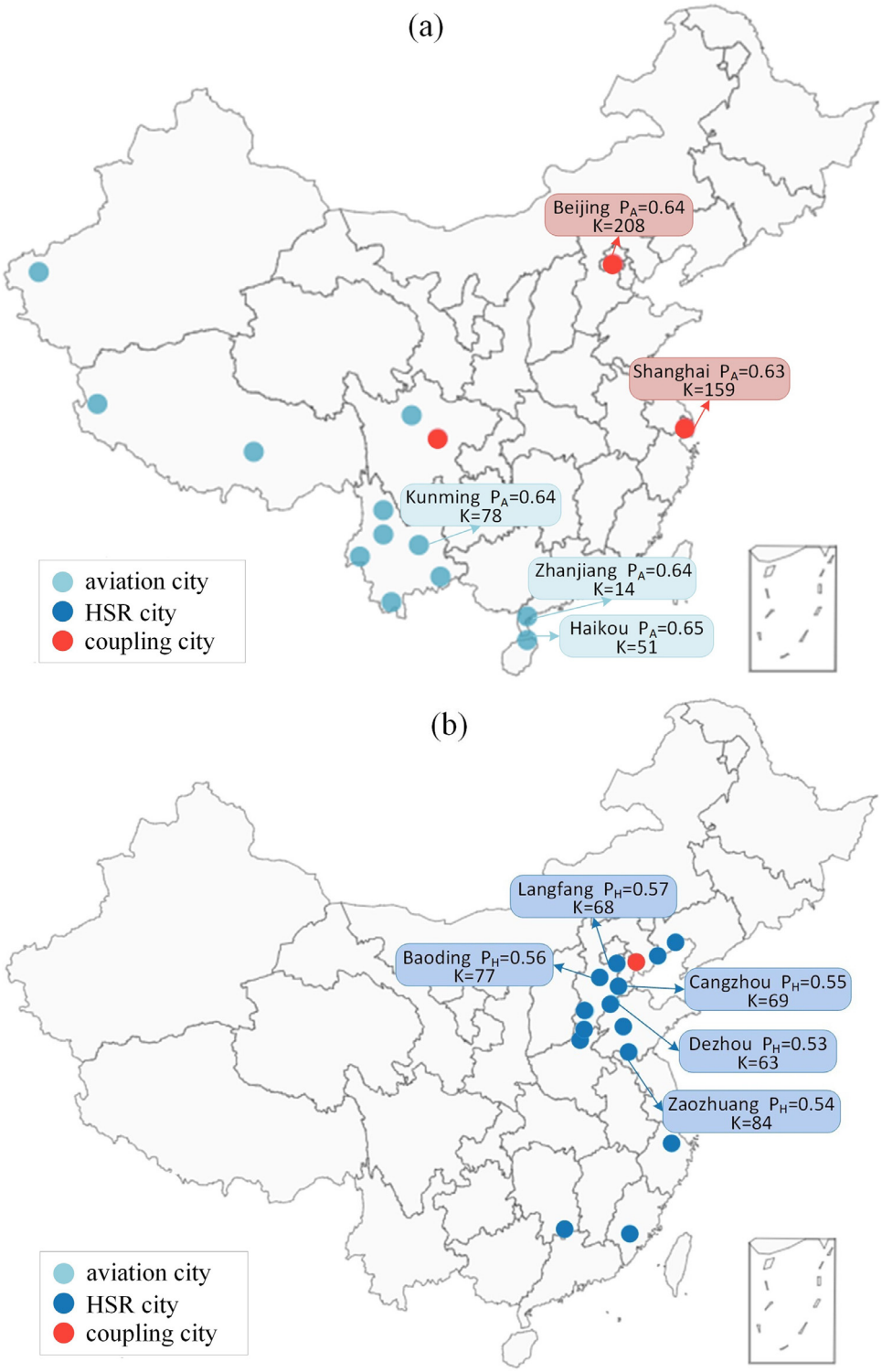

Fig. 9. (a) Fifteen cities with the highest p_A with the names and k values of the top five cities. (b) Fifteen cities with the highest p_H with the names and k values of the top five cities. Red dots are the coupling cities, light blue dots are the aviation cities, and dark blue dots are the HSR cities. (For interpretation of the references to color in this figure legend, the reader is referred to the web version of this article.).

the China National New-Type Urbanization Plan (2014–2020) [12]. Urban agglomeration planning also shows that different urban agglomerations are mainly connected by air through the core cities, while most of the other cities within the urban agglomeration are connected by high-speed rail. These results are consistent with urban agglomeration planning as passengers departing from these cities with high p_C usually need to arrive at a central city within the urban agglomeration by HSR first, and then use the central city as a transfer facility to their ultimate destinations. Therefore, the average number of transfers n of these cities is relatively large.

3.4.2. Analysis of robustness of the network

In order to reveal the air-HSR coupling relation, we conduct a robustness test of the flow of the CAHSR network [15]. Service in-

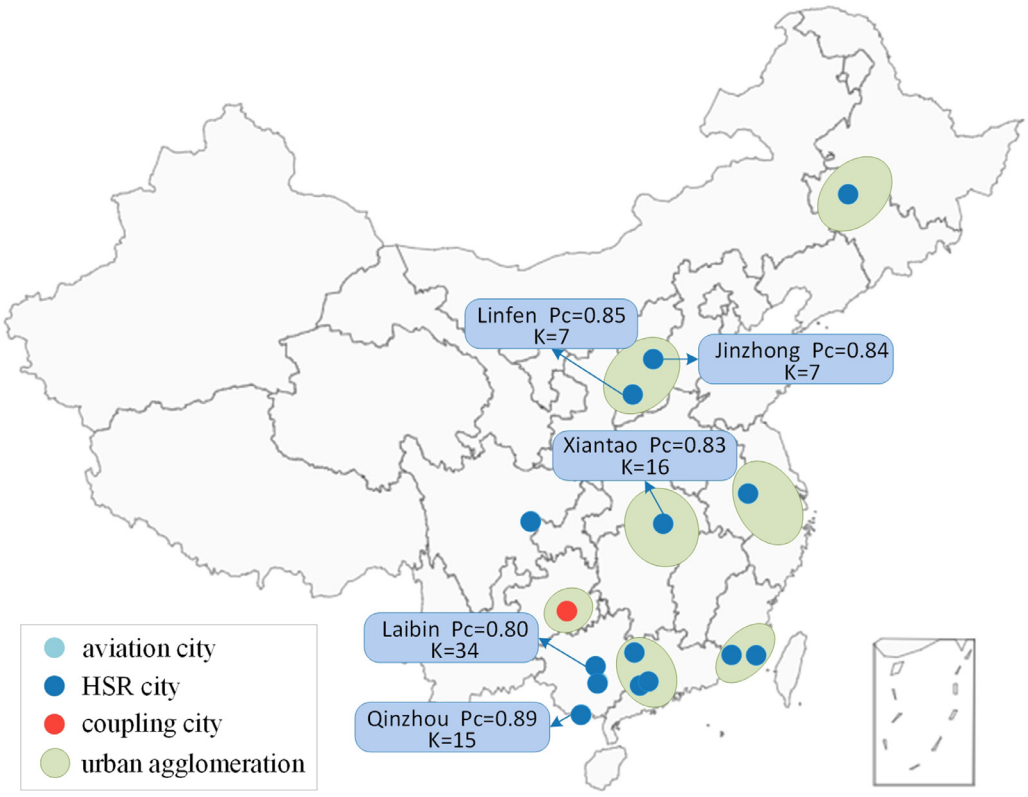

Fig. 10. Fifteen cities with the highest p_C with the names and k values of the top five cities. Red dots are the coupling cities, light blue dots are the aviation cities, and dark blue dots are the HSR cities. Green frames are urban agglomeration that the cities belong to. (For interpretation of the references to color in this figure legend, the reader is referred to the web version of this article.).

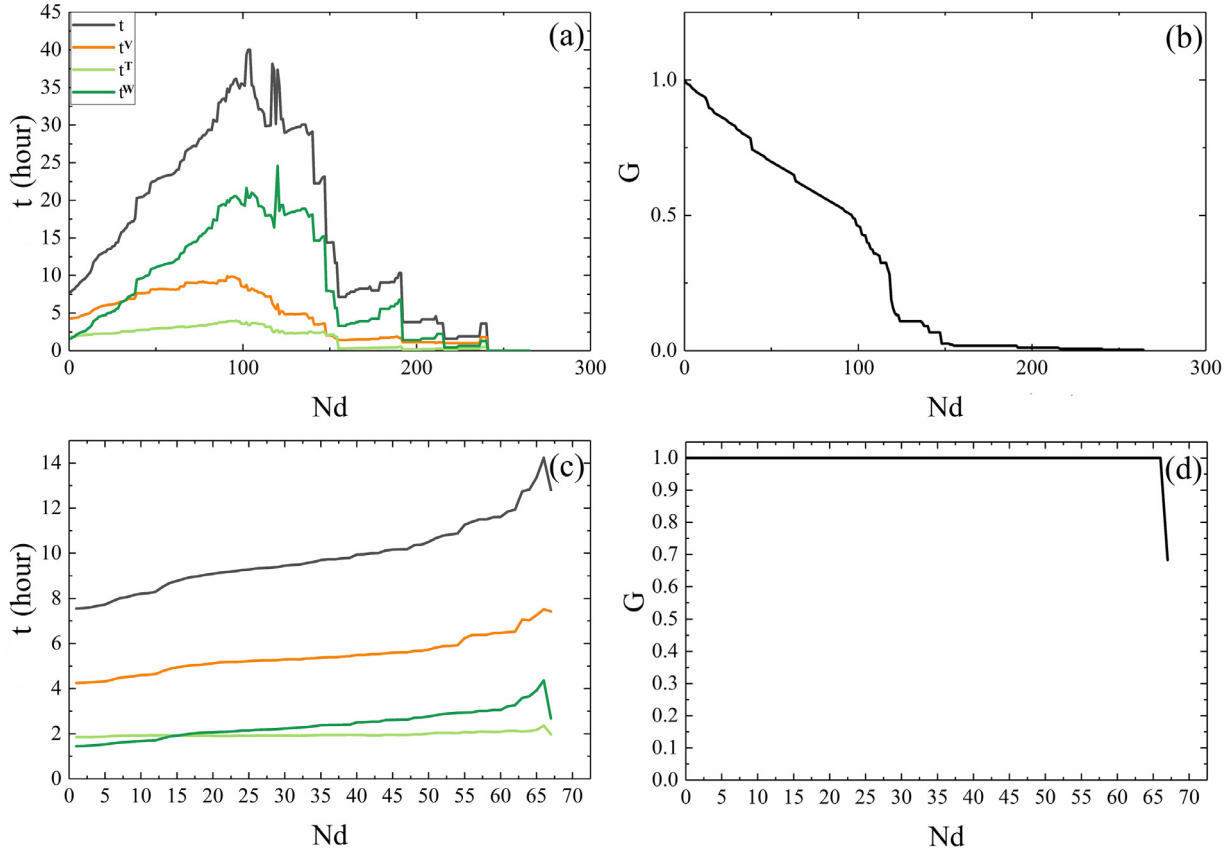

Fig. 11. (a) Travel time and (b) size of the largest connected component as functions of the number of cities *Nd* that have been removed from the network. (c) and (d) report the same quantities for case 2. In Fig. (a) and (b), we remove cites from the network following a high-degree selection strategy. In Fig. (c) and (d), we prevent transfers between airports and HSR stations in coupling cities. Black lines are the total travel time t, orange lines are flight/rail travel time t^V, light green lines are transfer time t^T, and dark green lines are waiting time t^W. (For interpretation of the references to color in this figure legend, the reader is referred to the web version of this article.).

terruption at an airport/HSR station may greatly affect the overall performance of the entire transport system. In particular, performance under transfer failures in coupling cities reflects the level of aviation-HSR cooperation to some extent. Therefore, we carry out experiments regarding two aspects.

1) Case 1: interruption of all air/HSR service in a city.
2) Case 2: interruption of air-HSR transfer in coupling cities.

In Case 1, the extreme case of sequentially shutting down airports/HSR stations, we implement interruption of all flights/HSR services of a city by removing that city from the CAHSR network following a high-degree selection strategy. Fig. 11(a) shows the changes in travel time as the number of removed cities Nd grows. At first, as removed cities are originally key transfer hubs in the network, the total travel time t rises rapidly. Afterwards, when the number of removed cities Nd exceeds 100, less than half of the cities remain connected with connected subgraph G=46% as shown in Fig. 11(b). With further reduction of the city number, the initial network is broken into several regional clusters, and city distances in each connected subgraph tend to be smaller. Consequentially, the overall time consumption starts to decrease sharply. Travel time components in-vehicle travel time t^V, transfer time t^T, and waiting time t^W all follow the same pattern of total travel time t. Specifically, waiting time t^W experiences the greatest change. When $Nd = 31$, t^W exceeds t^V, indicating that passengers spend more time waiting than traveling on flights/HSR.

In Case 2, we invalidate the ground transfers between different facilities (airports and/or HSR stations) within coupling cities following a high-degree selection strategy. As shown in Fig. 11(d), unlike Case 1, all cities still remain connected with connected subgraph G=1 before the ground transfer of the last coupling city fails. As more transfer failures occur in the network, an increasing number of passengers have to make detours to get to their destinations. As in Fig. 11(c), the total travel time rises steadily until reaching the last point Nd=67. When reaching the last point, the CAHSR network is divided into two subgraphs: the aviation layer and the HSR layer. Therefore, the average travel time of the network and G will decrease sharply. An interesting finding is that the average total travel time of the whole network almost doubles (from 7.55 h to 14.24 h) when there is only one intermodal city left. In brief, the cooperation of aviation and HSR plays a critical role in improving passengers' mobility.

4. Conclusions

In this paper, we have used network theory to model and study the Chinese aviation and high-speed rail network as a multi-layer coupled network. The cities in the CAHSR network are divided into three types, namely, aviation-only cities, HSR-only cities, and coupling cities, with coupling cities mainlypresent in eastern region of China. We have found that total travel time from coupling cities are significantly shorter, when compared to those from HSR-only cities and aviation-only cities. Moreover, we have considered variable departure time, at hourly intervals. The results show that changing the departure time in cities with high degrees/weights does not greatly affect total travel time. Finally, intermodal dependence and robustness properties of the CAHSR network have been investigated. The results in this case indicate that the cities with the highest dependence on the air-HSR intermodal transport are the small cities near municipalities and provincial capitals, and the majority of them are situated in urban agglomerations. A particularly interesting finding is that when only one coupling city exists in the CAHSR network, the average travel time of the whole network almost doubles from 7.55 to 14.24 h. In our future research, we will focus on the integration of aviation and HSR scheduling to reduce unnecessary waiting time at transfer airports/stations, such as flight/high-speed rail schedule optimization and integrated construction of air and high-speed rail infrastructure.

Declaration of Competing Interest

The authors declare that they have no known competing financial interests or personal relationships that could have appeared to influence the work reported in this paper.

CRediT authorship contribution statement

Yiqiao Wang: Conceptualization, Methodology, Software, Writing - review & editing. **Qiaoyi Lu:** Data curation, Validation, Visualization, Writing - original draft. **Xianbin Cao:** Resources, Supervision. **Xuesong Zhou:** Formal analysis, Supervision. **Vito Latora:** Formal analysis, Writing - review & editing. **Lu Carol Tong:** Methodology, Writing - review & editing. **Wenbo Du:** Investigation, Project administration, Funding acquisition.

Acknowledgments

The first author, second author, third author, sixth author and seventh author are supported by National Key Research and Development Program of China under Grant 2019YFF0301400 and National Natural Science Foundation of China (Grant Nos. 61671031, 61722102, 71801006, 61961146005).

Appendix

1) Degree k_i and weight w_i

The degree k_i of city i is the number of cities that can be accessed directly from city i, while the weight w_i of city i is the number of flights and HSR departing from city i. All the stations (including the origin), except for the last HSR stations, are considered to have a HSR departing from them.

2) Cumulative degree distribution $P(k)$ and cumulative weight distribution $P(w)$

The cumulative degree distribution refers to the proportion of nodes in the network whose degree is not less than k. Similarly, the cumulative weight distribution refers to the proportion of nodes in the network whose weight is not less than w.

3) Clustering coefficient C

The clustering coefficient C indicates the probability that two nodes of a network with a common neighbor are connected, quantifying the tendency of a node to form triangles. The node clustering coefficient C_i of node i is defined as in Eq. (A1), where E_i is the number of edges between the neighbors of, and k_i is the number of neighbors of i:

$$C_i = \frac{2E_i}{k_i(k_i-1)} \tag{A1}$$

The clustering coefficient C of a network is defined in Eq. (A2), where N is the number of nodes in the network.

$$C = \frac{1}{N}\sum_i C_i \tag{A2}$$

4) Average shortest path length L

The average shortest path length is the average length of the shortest path between all pairs of nodes in the network. L is defined in Eq. (A3), where l_{ij} is the length of the shortest path between nodes i and j.

$$L = \frac{2}{N(N-1)}\sum_{i,j\in N, i\neq j} l_{ij} \tag{A3}$$

5) Degree heterogeneity H

The degree heterogeneity is used to measure the difference of the degree of nodes in the network. It is defined in Eq. (A4), where k_i^2 denotes the average of k_i^2 and k_i denotes the average of k_i.

$$H = \frac{k_i^2}{k_i},\ i \in N \tag{A4}$$

6) Degree-degree correlation coefficient r

In order to study the presence of degree-degree correlation in the network, the network correlation coefficient r is defined in Eq. (A5), where k_e, k'_e are the degrees of the nodes at the ends of the eth edge, with $e = 1, 2, \ldots, E$.

$$r = \frac{M^{-1}\sum_e k_e k'_e - \left[M^{-1}\sum_e \frac{1}{2}\left(k'_e + k_e\right)\right]^2}{M^{-1}\sum_e \frac{1}{2}\left(k'^2_e + k^2_e\right) - \left[M^{-1}\sum_e \frac{1}{2}\left(k'_e + k_e\right)\right]^2} \tag{A5}$$

7) Betweenness centrality B_i

Betweenness centrality B_i represents the proportion of the shortest paths that contains the node i. B_i is defined in Eq. (A6), where g_{sj} is the number of the shortest paths from node s to node j and f_{sj} is the number of shortest paths in g_{sj} containing node i.

$$B_i = \sum_{s \neq i \neq j} \frac{f^i_{sj}}{g_{sj}} \tag{A6}$$

8) Density d

Density d represents the connectivity between nodes in a network, and is defined in Eq. (A7). The value range of network density is between 0 and 1. When d equals to 1, it indicates that the network is full-connected.

$$d = \frac{2k}{N(N-1)} \tag{A7}$$

References

[1] Albalate D, Bel G, Fageda X. Competition and cooperation between high-speed rail and air transportation services in Europe. J Transp Geogr 2015;42:166–74.
[2] Aleta A, Meloni S, Moreno Y. A multilayer perspective for the analysis of urban transportation systems[J]. Sci Rep 2017;7:44359.
[3] Boccaletti S, Bianconi G, Criado R, et al. The structure and dynamics of multilayer networks. Phys Rep 2014;544(1):1–122.
[4] Boccaletti S, Latora V, Moreno Y, et al. Complex networks: structure and dynamics. Phys Rep 2006;424(4–5):175–308.
[5] Battiston F, Nicosia V, Latora V. Structural measures for multiplex networks. Phys Rev E 2014;89(3):032804.
[6] Barabási AL, Albert R. Emergence of scaling in random networks. Science 1999;286(5439):509–12.
[7] Barrat A, Barthelemy M, Pastor-Satorras R, et al. The architecture of complex weighted networks[J]. Proc Natl Acad Sci 2004;101(11):3747–52.
[8] Buldyrev SV, Parshani R, Paul G, et al. Catastrophic cascade of failures in interdependent networks. Nature 2010;464(7291):1025.
[9] Bergantino AS, Capozza C, Capurso M. The impact of open access on intra-and inter-modal rail competition. A national level analysis in Italy. Transp Policy 2015;39:77–86.
[10] Barthélemy M. Spatial networks[J]. Phys Rep 2011;499(1–3):1–101.
[11] Cohen R, Havlin S. Complex networks: structure, robustness and function. Cambridge: University Press; 2010.
[12] Central committee of the Communist Party of China (CCCPC) and the State Council of the People's Republic of China (SCPRC), 2014. China National New-type Urbanization Plan (2014-2020). http://www.gov.cn/zhengce/2014-03/16/content_2640075.htm (accessed 16.03.2014). (in Chinese)
[13] Du WB, Zhou XL, Lordan O, et al. Analysis of the Chinese Airline Network as multi-layer networks. Transp Res Part E 2016;89:108–16.
[14] Du WB, Zhang MY, Zhang Y, et al. Delay causality network in air transport systems. Transp Res Part E 2018;118:466–76.
[15] De Domenico M, Solé-Ribalta A, Gómez S, et al. Navigability of interconnected networks under random failures[J]. Proc Natl Acad Sci 2014;111(23):8351–6.
[16] Guimera R, Mossa S, Turtschi A, et al. The worldwide air transportation network: anomalous centrality, community structure, and cities' global roles. Proc Natl Acad Sci 2005;102(22):7794–9.
[17] Goh KI, Lee DS, Kahng B, et al. Sandpile on scale-free networks[J]. Phys Rev Lett 2003;91(14):148701.
[18] Google Maps Platform, 2019. Distance Matrix API. https://developers.google.com/maps/documentation/distance-matrix/intro#optional-parameters (updated on 16.01.2019).
[19] Gallotti R, Barthelemy M. The multilayer temporal network of public transport in Great Britain[J]. Sci Data 2015;2(1):1–8.
[20] Gallotti R, Barthelemy M. Anatomy and efficiency of urban multimodal mobility[J]. Sci Rep 2014;4(1):1–9.
[21] Hong C, Zhang J, Cao XB, et al. Structural properties of the Chinese air transportation multilayer network. Chaos, Solitons & Fractals 2016;86:28–34.
[22] Jiang CM, Zhang AM. Effects of high-speed rail and airline cooperation under hub airport capacity constraint. Transp Res Part B 2014;60:33–49.
[23] Kurant M, Thiran P. Layered complex networks[J]. Phys Rev Lett 2006;96(13):138701.
[24] Latora V, Nicosia V, Russo G. Complex networks: principles, methods and applications. Cambridge University Press; 2017.
[25] Manfredi S, Di Tucci E, Latora V. Mobility and congestion in dynamical multilayer networks with finite storage capacity. Phys Rev Lett 2018;120(6):068301.
[26] Ministry of Transport of the People's Republic of China (MOT), 2019. Statistics of major production indicators of CAAC in December 2018. http://www.mot.gov.cn/tongjishuju/minhang/ (accessed 20.02.2019). (in Chinese)
[27] National Development and Reform Commission (NDRC) and Civil Aviation Administration of China (CAAC), 2017. National civil transport airport layout planning. http://www.ndrc.gov.cn/zcfb/zcfbghwb/201703/t20170315_841017.html (accessed 13.02.2017). (in Chinese)
[28] National Development and Reform Commission (NDRC), Ministry of Transport of the People's Republic of China (MOT) and China Railway Corporation (CR), 2017. Medium- and long-term railway network planning. http://ghs.ndrc.gov.cn/ghwb/gjgh/201705/U020170516620657922852.pdf (accessed 16.05.2017). (in Chinese)
[29] Newman MEJ. The structure and function of complex networks. SIAM Rev 2003;45(2):167–256.
[30] Newman MEJ. Networks: an introduction. Oxford University Press; 2010.
[31] Perra N, Goncalves B, Pastor-Satorras R, et al. Activity driven modeling of time varying networks[J]. Sci Rep 2012;2:469.
[32] Sen P, Dasgupta S, Chatterjee A, et al. Small-world properties of the Indian railway network[J]. Phys Rev E 2003;67(3):036106.
[33] Shao J, Buldyrev S V, Havlin S, et al. Cascade of failures in coupled network systems with multiple support-dependence relations. Phys Rev E 2011;83(3):036116.
[34] Sen P, Chakrabarti BK. Sociophysics: an introduction[M]. Oxford University Press; 2014.
[35] United Nations Development Program (NUDP), 2016. China National Human Development Report 2016. http://www.cn.undp.org/content/china/zh/home/library/human_development/china-human-development-report-2016.html (accessed 17.08.2016). (in Chinese)
[36] Van Mieghem P. Graph spectra for complex networks. Cambridge University Press; 2010.
[37] Wang Z, Andrews MA, Wu ZX, et al. Coupled disease–behavior dynamics on complex networks: a review. Phys Life Rev 2015;15:1–29.
[38] Watts DJ, Strogatz SH. Collective dynamics of 'small-world' networks. Nature 1998;393(6684):440.
[39] Watts DJ. A simple model of global cascades on random networks[J]. Proc Natl Acad Sci 2002;99(9):5766–71.
[40] Xia WY, Zhang AM. High-speed rail and air transport competition and cooperation: a vertical differentiation approach. Transp Res Part B 2016;94:456–81.
[41] Yang HR, Dobruszkes F, Wang JE, et al. Comparing China's urban systems in high-speed railway and airline networks. J Transp Geogr 2018;68:233–44.
[42] Zhu ZR, Zhang AM, Zhang YH. Connectivity of intercity passenger transportation in China: a multi-modal and network approach. J Transp Geogr 2018;71:263–76.
[43] Zhu ZR, Zhang AM, Zhang YH. Measuring multi-modal connections and connectivity radiations of transport infrastructure in China[J]. Transportmetrica A: Transport Science 2019;15(2):1762–90.